Research Article | Vol. 27, No. 26 / 23 December 2019 / Optics Express 38579
Optics EXPRESS

Chromatic dispersion mitigation using a SEFDM-based diversity technique for IM/DD long reach optical links

BAOXIAN YU,[1,2] CHANGJIAN GUO,[3,4,7] SEN ZHANG,[5] TIANJIAN ZUO,[5] LEI LIU,[5] ALAN PAK TAO LAU,[6] CHAO LU,[4] AND HAN ZHANG[1,2,8]

[1]*Department of Physics and Telecommunication Engineering, South China Normal University, Guangzhou, China*
[2]*Guangdong Provincial Engineering Technology Research Center of Cardiovascular Individual Medicine & Big Data, South China Normal University, Guangzhou, China*
[3]*South China Academy of Advanced Optoelectronics, South China Normal University, Guangzhou, China*
[4]*Photonics Research Center, Department of Electronic and Information Engineering, The Hong Kong Polytechnic University, Hong Kong, China*
[5]*Network Technology Laboratory, Huawei Technologies Co., Ltd., Shenzhen, China*
[6]*Photonics Research Center, Department of Electrical Engineering, The Hong Kong Polytechnic University, Hong Kong, China*
[7]*changjian.guo@coer-scnu.org*
[8]*zhanghan@scnu.edu.cn*

Abstract: Spectral efficient frequency division multiplexing (SEFDM) can offer a higher spectral efficiency (SE) than orthogonal frequency division multiplexing (OFDM). In this work, we propose a diversity technique based on SEFDM for beyond 100-Gb/s optical intensity modulation and direct detection (IM/DD) long reach (LR) applications. We mathematically demonstrate that the self-created inter-carrier interference of SEFDM signals can be reused to achieve a diversity gain on each sub-carrier and, in turn, improve the tolerance to power fading induced by chromatic dispersion (CD) in IM/DD LR links. Based on the proposed diversity technique, we further demonstrated a 112-Gb/s SEFDM transmission over 80-km standard single-mode fiber, using only 28-GHz bandwidth and modulation format of up to 16-QAM. Experimental results show that SEFDM with the proposed diversity technique performs robust against CD effects and outperforms the conventional OFDM with adaptive bit and power loading of the same bandwidth and data rate, which validates the superiority of the proposed SEFDM in optical IM/DD LR transmissions.

1. Introduction

For long reach (LR) applications, such as LR passive optical networks and LR inter-datacenter optical inter-connects, intensity modulation and direct detection (IM/DD) are more desirable than coherent schemes owing to the simple implementations and low costs [1–3]. In IM/DD systems, double side-band (DSB) modulation suffers from power fading induced by chromatic dispersion (CD), especially for the case of either long transmission distance or wide signal bandwidth [4]. To mitigate the CD effects, many techniques have been proposed, namely, Kramers-Kronig receiver, single side-band modulation, CD pre-compensation, block-wise phase switching, etc [5–11]. However, the above-mentioned methods entail either extra resource or complicated transmitter configurations, which may actually limit the effective payloads [12].

Orthogonal frequency division multiplexing (OFDM) [13] has been widely considered in LR optical links to achieve both higher data rate and spectral efficiency (SE) [14,15], since it can benefit from flexible modulation by integrating with adaptive bit and power loading

#381267 https://doi.org/10.1364/OE.381267
Journal © 2019 Received 31 Oct 2019; revised 4 Dec 2019; accepted 8 Dec 2019; published 19 Dec 2019

Optics EXPRESS

(ABPL) [16–18]. Recently, spectrally efficient frequency division multiplexing (SEFDM), as an alternative discrete multi-tone (DMT) technology, received extensive attentions in optical communications due to its potential of improving SE in comparison with OFDM [19–23]. Similar to OFDM, SEFDM is robust to inter-symbol interference (ISI) with the aid of zero-padded guard interval (GI) [24]. It has also been reported that SEFDM can take advantage of the self-introduced inter-carrier interference (ICI) and enjoy a better immunity against the power fading under CD channels [25]. As a consequece, SEFDM has the potential in the application of high speed LR optical links.

In this work, we study the problem of SEFDM for LR transmissions, and propose a diversity technique with adaptive bit loading to mitigate the CD effects, while achieving a higher data rate. The motivation behind the proposed scheme is that, SEFDM can take advantage of cross talk on adjacent sub-carriers by using the principle of maximum ratio combining (MRC), and in turn, achieves a diversity gain on each sub-carrier. Through mathematical analysis, we show that SEFDM with the proposed diversity technique can provide better tolerance to power fading in comparison with OFDM. Furthermore, we successfully demonstrated a 112-Gb/s SEFDM IM/DD transmission over 80-km of standard single-mode fiber (SSMF) with simplified bit loading, where a modulation up to 16-QAM was employed with only 28-GHz bandwidth. Experimental results show that SEFDM with the proposed diversity technique outperforms the conventional OFDM with adaptive bit and power loading of the same bandwidth and bit rate for LR applications.

2. Operating principle

2.1. SEFDM system model

As has been elaborated in [19], SEFDM is in principle a non-orthogonal DMT technology, where the frequency-domain symbols $S_k, k = 1, 2, \ldots, N$ are modulated on sub-carriers in the conjugate symmetry property as

$$S_{N_f-k} = S_k^*, \tag{1}$$

where N and $N_f \geq 2N + 2$ denote SEFDM symbol-size and the size of fast Fourier transform (FFT), respectively, and superscript * stands for the conjugate operation. For the index of sub-carriers without carrying information signals, i.e., $k = 0, N + 1, N + 2, \ldots, N_f - N - 1$, zeros are padded for ease of performing an N_f-point inverse FFT (IFFT), and the resulting real-valued time-domain signals are given by

$$x_n = \sum_{k=0}^{N_f-1} S_k \exp\left(\frac{j2\pi kn}{N_f}\right), n = 0, 1, \ldots, N_f - 1. \tag{2}$$

Compared with OFDM, where all the outputs after IFFT are transmitted to guarantee the orthogonality among sub-carriers, SEFDM can improve the SE and data rate by shortening the signal duration [19]. To elaborate a little further, SEFDM transmits only the first $N_1 \leq N_f$ IFFT results, and thus, the bandwidth compression factor (BCF) of SEFDM is defined by

$$\alpha = \frac{N_1}{N_f}. \tag{3}$$

For constellations with a cardinality of M, e.g., M-QAM, the SE of OFDM and SEFDM are respectively given by

$$\eta_O = \log_2 M, \tag{4}$$

and

$$\eta_S = \frac{\log_2 M}{\alpha}. \tag{5}$$

From above, SEFDM can achieve a higher SE of $(1 - \alpha)/\alpha \times 100\%$ in comparison with OFDM. In particular, SEFDM is identical to OFDM only when $\alpha = 1$.

Optics EXPRESS

Consider LR optical fiber channels, the quasi-static channel response reads

$$H_k = \cos\left(\frac{4\pi LD(k\lambda f)^2}{cN_f^2}\right), k = 1, 2, \ldots, N \tag{6}$$

where L and D denotes the length of fiber and CD value, respectively, λ is the center wavelength, f and c stand for signal bandwidth and speed of light in vacuum, respectively.

Similar to OFDM, SEFDM employs a GI in time-domain to avoid ISI prior to transmission, as illustrated in Fig. 1. At the receiver, the FFT outputs read [24]

$$Y_k = H_k W_{k,k} S_k + H_k \sum_{i=1, i\neq k}^{N} W_{k,i} S_i + Z_k, \tag{7}$$

where Z_k denotes zero-mean additive white Gaussian noise (AWGN) with a variance of $\alpha\sigma^2$, and

$$W_{k,i} = \frac{1}{N_f} \sum_{n=0}^{N_1-1} \exp\left(\frac{-j2\pi n(k-i)}{N_f}\right), \tag{8}$$

where $W_{k,i}, k = i$ and $k \neq i$ denote the weighted factors of the desired symbol and ICI, corrsponding to the first and the second items on right-hand-side of (7), respectively. It is noted that ICI of SEFDM is raised by the loss of orthogonality among sub-carriers, which is different from OFDM.

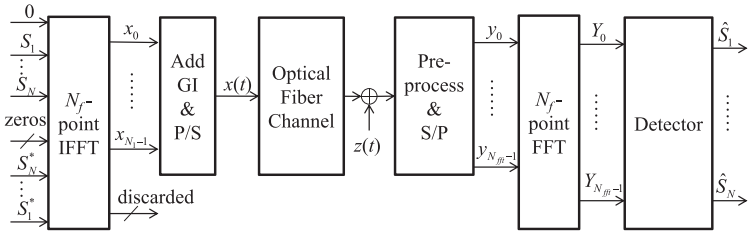

Fig. 1. SEFDM transceiver diagram.

2.2. *Proposed diversity technique*

Motivated by [25], we notice that SEFDM can achieve a diversity gain on a specific sub-carrier by taking advantage of the resulting signals after ICI cancellation. In this paper, we further elaborate the principle.

Recall (7) and employ decision-feedback for ICI cancellation [26], the received signal of S_k dispersed on n^{th} sub-carrier can be given by

$$\begin{aligned} Y_{n,k} &= Y_n - H_n \sum_{i=1, i\neq k}^{N} W_{n,i} \tilde{S}_i \\ &= H_n W_{n,k} S_k + \Delta_n + Z_n, \end{aligned} \tag{9}$$

where Δ_n denotes the residual interference induced by decision-feedback, i.e.,

$$\Delta_n = H_n \sum_{i=1, i\neq k}^{N} W_{n,i}(S_i - \tilde{S}_i), \tag{10}$$

where $\tilde{S}_i$ stands for the initial detection of S_i.

Optics EXPRESS

In this case, an N-dimensional vector $\{Y_{n,k}\}$ can be jointly considered for the decision on S_k, and thereby, MRC can be adopted to achieve a diversity gain on a specific sub-carrier, i.e.,

$$\begin{aligned}\hat{S}_k &= \frac{\sum_{n=1}^{N} H_n^* W_{n,k}^* Y_{n,k}}{\sum_{n=1}^{N} \left|H_n W_{n,k}\right|^2} \\ &= S_k + \frac{\hat{Z}_k}{G_k},\end{aligned} \tag{11}$$

where $\hat{Z}_k$ denotes the equivalent interference after MRC.

$$\hat{Z}_k = \frac{\sum_{n=1}^{N} H_n^* W_{n,k}^* (\Delta_n + Z_n)}{\sqrt{\alpha \sum_{n=1}^{N} \left|H_n W_{n,k}\right|^2}}, \tag{12}$$

and

$$G_k = \sqrt{\frac{\sum_{n=1}^{N} \left|H_n W_{n,k}\right|^2}{\alpha}}. \tag{13}$$

Clearly, the optical fiber channel response at k-th sub-carrier after MRC, i.e., G_k in (13), is in fact the weighted channel response of H_k (without MRC) in (6) over whole sub-carriers.

In general, the performance of detection in (11) depends on the frequency selectivity of channel response, i.e., $\mathrm{var}\{|G_k|^2\}$, where $\mathrm{var}\{\cdot\}$ denotes the variance [24]. To be specific, the smaller the variance of $|G_k|^2$ is, the better the performance of detection in (11) can be obtained.

Proposition 1 *For SEFDM with MRC, the frequency selectivity of channel response* $\mathrm{var}\{|G_k(\alpha_1)|^2\}$ *is directly proportional to* α.

Proof: See Appendix.

From *Proposition* 1 and (13), we have $\mathrm{var}\{|G_k(\alpha)|^2\} < \mathrm{var}\{|G_k(1)|^2\} = \mathrm{var}\{|H_k|^2\}, \forall \alpha < 1$, which indicates that the equivalent channel response G_k is more 'flat' than that of H_k by taking advantages of MRC. This conclusion is identical to that of [24], where the latter is a special case of *Proposition* 1.

Ideally, as α decreases from 1 to 0, SEFDM can benefit more from the proposed diversity technique using MRC in (11). In the case of small α or low signal-to-noise ratio (SNR), however, the residual ICI Δ_n might significantly degrade the performance. Nevertheless, for practical ranges of $\alpha \geq 0.6$ [27,28] in high SNR scenarios, the maximum likelihood (ML) detection can be adopted to remove ICI favorably, and in turn, yield an improvement of ultimate performance in comparison with OFDM.

We carried out simulations to validate the above expectations, where symbol-size and FFT size of SEFDM are $N = 62$ and $N_f = 128$, respectively. For simplicity, 4-QAM modulation is considered. We set $N_1 = 96$ and $N_1 = 102$ to perform SEFDM with $\alpha = 0.75$ and $\alpha = 0.80$, respectively, and the signal bandwidth is fixed as 28-GHz. Besides, an 80-km SSMF link with center wavelength of 1550.12-nm and CD value of 16-ps/(nm·km) is considered. In this work, we employ the log-MAP Viterbi decoding method to remove ICI [19].

Figure 2(a) compares the channel response of an 80-km SSMF link with and without MRC, which corresponds to G_k and H_k, repectively. As shown in Fig. 2(a), the former can benefit significantly from the diversity gain of whole sub-carriers, and is indeed more 'flat' than the latter. Clearly, the result is consistent with *Proposition* 1 and the analysis therein. Specifically, a maximum gain of 30dB in channel response can be reached, which indicates that the proposed SEFDM-based diversity technique can effectively mitigate the frequency selectivity in CD channels.

In addition, we evaluated the performance comparison between SEFDM with the proposed diversity technique and OFDM over 80-km SSMF with AWGN. Note that the system parameters

Optics EXPRESS

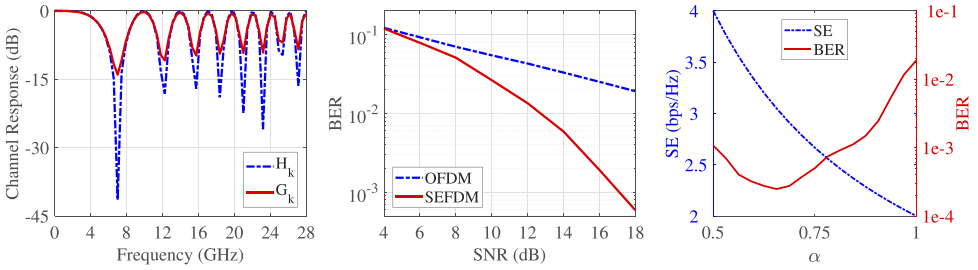

(a) (b) (c)

Fig. 2. (a) Simulated channel response of the proposed SEFDM with $\alpha = 0.80$ through an 80-km SSMF link. (b) Simulated BER performance of the SEFDM with the proposed diversity technique at $\alpha = 0.75$ using 4-QAM modulation in 80-km CD channel. (c) BER and SE at various BCFs when SNR=18dB.

of SEFDM and OFDM are totally the same, and both use 4-QAM constellation. Figure 2(b) shows the bit error rate (BER) performance of the proposed scheme with $\alpha = 0.75$ in comparison with OFDM. Clearly, SEFDM outperforms OFDM attributed to the diversity gain, while yielding a spectral gain of 33.33% simultaneously.

We also examined the effect of BCF on the performance of the proposed SEFDM. As illustrated in Fig. 2(c), SE of the proposed SEFDM is inversely proportional to the BCF, which corresponds to (5), while BER is a convex function of α. To be specific, the BER performance is enhanced at the early stage and then degrades as BCF decreases, and the best performance is achieved at $\alpha \approx 0.65$. This is reasonable by *Proposition* 1 and corresponding analysis that SEFDM with smaller BCF benefits more from diversity gain with slight noise amplification when $\alpha > 0.65$. However, in the case of $\alpha < 0.65$, the performance degradation resulted from the noise amplification is more significant than the diversity gain due to the increment of residual ICI. As a consequence, we can conclude from Fig. 2(c) that there is a trade-off between SE and BER performance, and a moderate BCF is recommended for the proposed scheme.

3. Experimental setup

The experimental setup is shown in Fig. 3. Based on extensive simulations, a moderate FFT size ranging from 64 to 256 is recommended. The SEFDM signals were generated offline. Specifically, in order to generate the real-valued SEFDM signal, data were modulated on $2^{nd} - 63^{rd}$ sub-carriers and mapped conjugate symmetrically into $67^{th} - 128^{th}$ ones, while the other sub-carriers were zero-padded. After IFFT, the last $N_f - N_1$ time-domain samples were discarded to form a SEFDM block, which was padded with GI of 32-point zeros to mitigate inter-block interference. Note that cyclic prefix may be no longer suitable for SEFDM due to the loss of orthogonality among sub-carriers, while zero-padded GI can formulate a circulant structure to facilitate a one-tap frequency domain equalization [24]. The occupied bandwidth of the generated signals in this work was 28-GHz, since the sample rate was set to 56-Gsa/s. After parallel/serial (P/S) conversion, 1920 blocks of SEFDM signals as well as the pilot signals, including one block of timing synchronization pattern and 128 blocks of OFDM training sequences were up-sampled to 100-Gsa/s using digital linear interpolation. To avoid high peak-to-average power ratio issue, clipping technique was considered as in [29]. The whole signals were then loaded into a digital-to-analog converter (DAC) operating at f_s=100-Gsa/s, before modulated through a Mach Zehnder modulator (MZM) to form the DSB signals. The optical carrier used in this experiment had a center wavelength of 1550.12-nm. After 80-km SSMF transmission, a variable optical attenuator (VOA) was used to adjust the received optical power (ROP) before an Erbium doped

Optics EXPRESS

fiber amplifier (EDFA) with a noise figure of about 4.3-dB. The optical signals were filtered and then detected by a photo-diode (PD) with a bandwidth of 43-GHz. The electrical signals after PD were digitized by a 160-Gsa/s real time oscilloscope and then processed off-line. The main off-line DSP procedures include timing synchronization, serial/parallel (S/P) conversion, GI processing followed by FFT, channel estimation and equalization, as well as detection using our log-MAP Viterbi decoding scheme with 32 surviving paths.

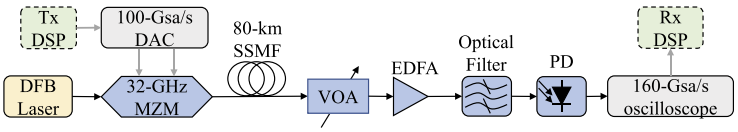

Fig. 3. Experimental setup.

For reference, we also conducted experiments on conventional ABPL-OFDM since it has been widely applied to LR optical links [30]. The systematic parameters are shown in Table 1. For fairness of comparison, both ABPL-OFDM and SEFDM signals used the same bandwidth and the same bit rates. To be spcific, the bit allocations of ABPL-OFDM are determined by both the bit rates of the proposed SEFDM and Chow's algorithm [31], and the contellation alphabet ranges from 4-QAM to 128-QAM. Note that Chow's algorithm can achieve a more flexible and precise ABPL using more sub-carriers in a fixed bandwidth, and in turn, yield a better performance. Hence, the FFT size of ABLP-OFDM was increased to 1024, with $N = 288$ sub-carriers modulating data symbols, where the signal bandwidth is $\frac{288}{1024} f_s = 28.125$-GHz.

Table 1. Systematic Parameters Used for Experiments

Parameter	N	N_f	N_1	α	f	constellations
SEFDM	62	128	96, 102	0.75, 0.80	28-GHz	4-QAM, 16-QAM
OFDM	288	1024	1024	1	28.125-GHz	up to 128-QAM

4. Results and discussions

We first explored the B2B performance of both the proposed SEFDM and the conventional ABPL-OFDM. 16-QAM symbols were modulated in 62 sub-carries of SEFDM with BCF of 0.75 since no fadings exist in B2B scenarios, while ABPL-OFDM employed Chow's algorithm [31] for bit allocations to achieve the same bit rate of 150-Gb/s. As shown in Fig. 4, both schemes achieve similar performance, while the proposed SEFDM yields a receiver sensitivity improvement of 1.5dB at the hard-decision forward error correction (HD-FEC) limit (BER = 3.8e-3). This fact is attributed to the lower constellation cardinality of the proposed SEFDM in limited SNR cases.

We then employed a simplied bit loading scheme for SEFDM to increase the bit rate according to the measured SNR after 80-km SSMF transmission. To be specific, we considered 4-QAM and 16-QAM modulations and set a variable SNR margin to determine the bit allocations for all sub-carriers. Note that higher order modulations can also be used, however, 16-QAM is sufficient to achieve a bit rate of 112-Gb/s in the following experiments thanks to the higher SE of SEFDM. Combining with various values of BCF, the corresponding bit rates can be illustrated in Table 2. For example, when SNR margin was set as 18-dB, 16-QAM was modulated on 26 sub-carriers with SNR $\geq$18-dB, otherwise 4-QAM was employed.

Next, we evaluated the performance of the proposed diversity technique of SEFDM with fixed BCF $\alpha = 0.75$ through 80-km SSMF transmissions. As shown in Fig. 5(a) and Table 2, the data rate grows as the SNR margin decreases, while suffering a performance degradation. This fact is

Optics EXPRESS

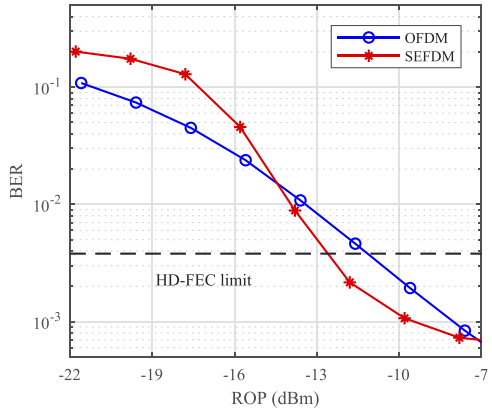

Fig. 4. B2B performance of the proposed SEFDM and ABPL-OFDM.

Table 2. Bit allocations and bit rates using the simplified bit loading scheme

SNR Margin (dB)	16.0	16.5	17.0	17.0	18.0	18.5
number of 16-QAM	36	34	30	30	26	20
number of 4-QAM	26	28	32	32	36	42
BCF	0.80	0.75	0.75	0.80	0.75	0.80
Raw bit rate (Gb/s)	107.19	112.00	107.33	100.63	102.67	89.69

expected since more 16-QAM symbols are used in small SNR margin cases. Nevertheless, ROP of no more than −12.8dBm can be achieved at the HD-FEC limit in 112-Gb/s case.

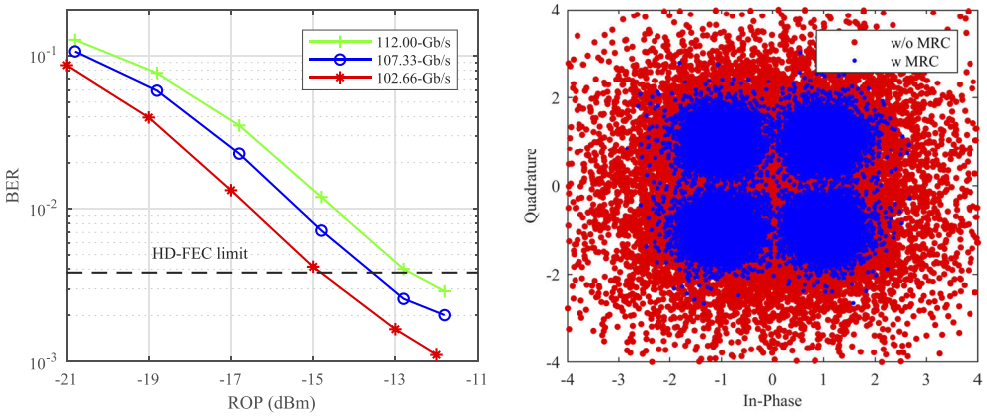

(a) (b)

Fig. 5. (a) BER performance of the proposed diversity technique using SEFDM with $\alpha = 0.75$ after 80-km SSMF transmission for various bit rates. (b) Estimated 4-QAM signal distributions with and without MRC.

In order to validate the effectiveness of the SEFDM-based diversity technique, Figure 5(b) shows the distributions of the estimated 4-QAM signals with and without MRC in 112-Gb/s case at ROP of −11.8dBm. Clearly, the signal distribution with MRC in (11) is much more distinguishable, which indicates the robust tolerance to CD effects of the proposed scheme.

Optics EXPRESS

We then explored the effect of BCF to the diversity performance in SEFDM systems. For fairness of comparison, bit rates of approximate 107.19-Gb/s and 107.33-Gb/s were considered with $\alpha = 0.80$ and $\alpha = 0.75$, respectively. As shown in Fig. 6, SEFDM with $\alpha = 0.75$ outperforms that with $\alpha = 0.80$. This fact is reasonable since a smaller BCF can benefit more from the diversity gain and mitigate the CD effects more efficiently.

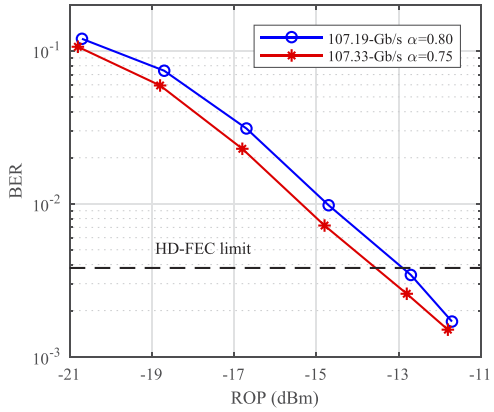

Fig. 6. BER performance of the proposed diversity technique using SEFDM after 80-km SSMF transmission at approximate bit rates with various BCFs.

To gain an insight into the performance of the proposed SEFDM-based diversity technique at various BCFs, Figs. 7(a) and 7(b) plot the measured SNR with and without MRC at $\alpha = 0.80$ and $\alpha = 0.75$, respectively. We can see that the maximum SNR improvement reaches 11.5-dB when $\alpha = 0.80$, while a 12.2-dB SNR gain can be achieved in case of $\alpha = 0.75$ with a SNR penalty of up to 2.38-dB in high SNR scenarios. The above results are expected and consistent with simulations and corresponding analysis, i.e., reducing BCF can improve the immunity to power fading while suffering from noise amplification due to the increased level of ICI. This leads to SNR degradation, especially for high order modulations. Based on extensive simulations and experiments, an appropriate range of BCF from 0.75 to 0.80 is recommended for the simplified bit loading scheme with modulation order up to 16-QAM.

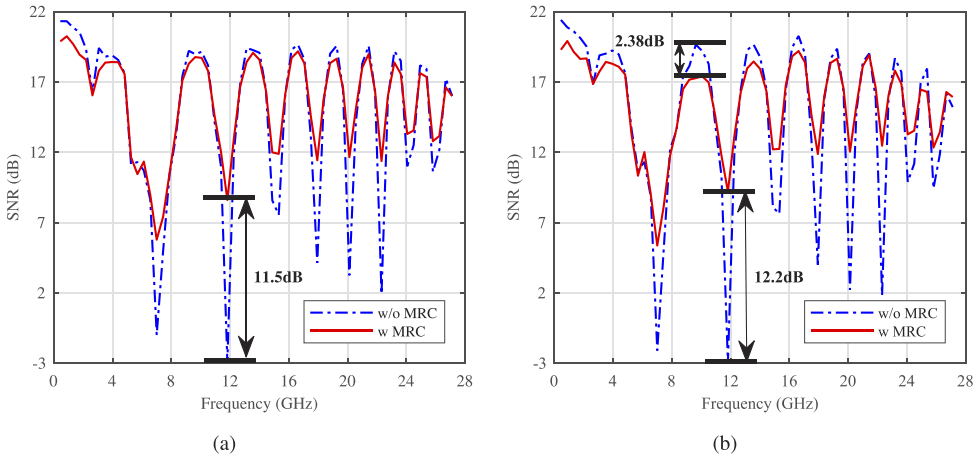

Fig. 7. Comparison between the measured receiver SNR with and without MRC. (a) $\alpha = 0.80$. (b) $\alpha = 0.75$.

Optics EXPRESS

We further demonstrated the performance comparison between SEFDM with the proposed diversity technique and the conventional ABPL-OFDM through 80-km SSMF. As shown in Fig. 8(a), the proposed SEFDM achieves a significant improvement of receiver sensitivity compared with OFDM at the HD-FEC limit, where both schemes achieve the same bit rate of 112-Gb/s using 28-GHz bandwidth. This is attributed to the diversity gain that improves the receiver SNR in the fadings, as well as low-order modulations (up to 16-QAM) that guarantees the favorable performance.

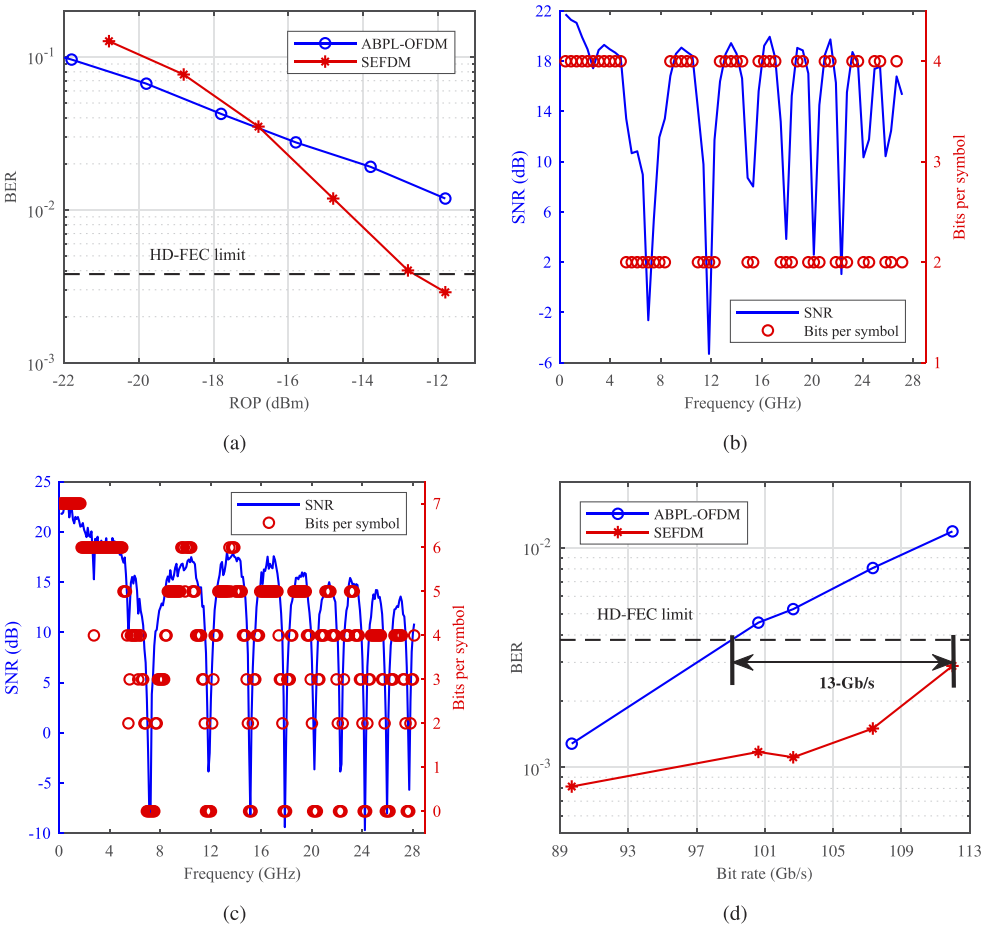

Fig. 8. (a) BER comparison between SEFDM with the proposed diversity technique and ABPL-OFDM at a bit rate of 112-Gb/s. (b) Measured systematic SNR and bit allocations of SEFDM. (c) Measured systematic SNR and bit allocations of OFDM. (d) BER performance of both schemes at a ROP of −11.8dBm.

In addition, the measured SNR and bit allocations of the proposed SEFDM and ABPL-OFDM are depicted in Figs. 8(b) and 8(c), respectively. Thanks to the diversity gain, SEFDM can modulate symbols in the whole 28-GHz band, even in those suffering from power fading induced by CD, which improves the effective payloads. On the contrary, ABPL-OFDM has to abandon sub-carriers with relatively low SNR, otherwise it might significantly degrades the ultimate performance. As a consequence, more bits should be allocated on the other sub-carriers to achieve the target bit rate, which requires high SNR to enable high-order constellations. In

Optics EXPRESS

practice, however, SNR is limited, where SEFDM with simplified bit loading scheme shows the competence.

Finally, we evaluated the performance of both schemes at various bit rates. As shown in Fig. 8(d), SEFDM with the proposed diversity technique outperforms ABPL-OFDM at the same bit rates, and performs fairly robust to the bit rate. In the case of HD-FEC limit, the proposed SEFDM yields more than 12% increment of bit rate in comparison with ABPL-OFDM. All the results above validate the superiority of the proposed SEFDM.

5. Conclusion

We have experimentally demonstrated an optical SEFDM IM/DD LR transmission, which can achieve a higher SE while offering a superior performance against the CD-induced power fading effects in comparison with OFDM. To mitigate the power fading, we proposed a diversity technique by taking advantage of ICI dispersion across adjacent sub-carriers based on MRC. We further performed simplified bit loading and the log-MAP Viterbi decoding to guarantee the bit rate and ML performance, respectively. We show through simulations that the proposed diversity technique can effectively reduce the effect of power fading on sub-carriers, and thereby, significantly improves the systematic SNR. In experimental study, we successfully demonstrated a 112-Gb/s SEFDM IM/DD transmission over 80-km SSMF with the proposed diversity technique, using only 28-GHz bandwidth and up to 16-QAM modulation. Under the same SE and bit rate, the proposed SEFDM outperforms the conventional ABPL-OFDM, which indicates the superiority of SFEDM in LR applications.

Appendix: proof of Proposition 1

Proposition 1 can be charaterized by

$$\mathrm{var}\{|G_k(\alpha_1)|^2\} \geq \mathrm{var}\{|G_k(\alpha_2)|^2\}, \forall \alpha_1 > \alpha_2, \tag{14}$$

where

$$\mathrm{var}\{|G_k(\alpha)|^2\} = \sum_{k=0}^{N_f-1} |G_k(\alpha)|^4 - \mu^2(\alpha), \tag{15}$$

where $\mu(\alpha)$ denotes the mean of $\{|G_k(\alpha)|^2\}$.

It has been demonstrated in [24] that $\mu(\alpha_i) = \mu(\alpha_j), \forall i, j$, and thereby, (14) is identical to

$$\sum_{k=0}^{N_f-1} |G_k(\alpha_1)|^4 \geq \sum_{k=0}^{N_f-1} |G_k(\alpha_2)|^4. \tag{16}$$

Due to the circulant property of $\{W_{n,k}\}$, recall (13) that

$$|G_k|^2 = \frac{|W_{0,k}|^2}{\alpha} \otimes |H_k|^2, \tag{17}$$

where $\otimes$ denotes circulant convolution. As will be elaborated in *Lemma* 1 and *Lemma* 2, $\sum_{k=0}^{N_f-1} |G_k(\alpha_1)|^4$ is propotional to the variance of weights $\left\{\frac{|W_{0,k}|^2}{\alpha}\right\}$.

Lemma 1 *Larger α results in larger variance of the weights $\frac{|W_{0,k}|^2}{\alpha}, k = 0, 1, \ldots, N_f - 1$, i.e., $\forall \alpha_1 > \alpha_2$, we have*

$$\sum_{k=0}^{N_f-1} \left| \frac{|W_{0,k}(\alpha_1)|^2}{\alpha_1} \right|^2 > \sum_{k=0}^{N_f-1} \left| \frac{|W_{0,k}(\alpha_2)|^2}{\alpha_2} \right|^2, \tag{18}$$

where $W_{0,k}(\alpha_1)$ and $W_{0,k}(\alpha_2)$ denote $W_{0,k}$ at α_1 and α_2, respectively.

Optics EXPRESS

Proof: Define $\mathbf{w}_1$ and $\mathbf{w}_2$ as the N_f-dimension IDFT results of $\{W_{0,k}\}$ and $\{W_{0,k}^*\}$, respectively, we have

$$\mathbf{w}_1 = \frac{1}{\sqrt{N_f N_1}}[1, \ldots, 1, 0, \ldots, 0]^T, \tag{19}$$

and

$$\mathbf{w}_2 = \frac{1}{\sqrt{N_f N_1}}[1, 0, \ldots, 0, 1, \ldots, 1]^T, \tag{20}$$

where the numbers of 1 and 0 are N_1 and $N_f - N_1$, respectively. Define $\mathbf{w} = \mathbf{w}_1 \otimes \mathbf{w}_2$, and thus, the n-th element of $\mathbf{w}$ reads

$$w_n = \frac{1}{N_f N_1} \max\left(\left|n - \frac{N_f}{2}\right| + N_1 - \frac{N_f}{2}, 2N_1 - N_f, 0\right). \tag{21}$$

Recall that $N_1 = \alpha N_f$, we can rewrite (21) as a function of α

$$w_n(\alpha) = \frac{1}{N_f} \max\left(1 - \frac{\beta}{\alpha}, 2 - \frac{1}{\alpha}, 0\right) \tag{22}$$

where

$$\beta = \begin{cases} 1 - \frac{n}{N_f} & n \geq \frac{N_f}{2} \\ \frac{n}{N_f} & n < \frac{N_f}{2} \end{cases}. \tag{23}$$

Obviously, $w_n(\alpha)$ is a monotonically increasing function of α, i.e., $\forall \alpha_1 > \alpha_2$, we have

$$w_n(\alpha_1) > w_n(\alpha_2). \tag{24}$$

In the light of Parseval's theorem, we have

$$\sum_{k=0}^{N_f-1} \left|\frac{|W_{n,k}(\alpha_1)|^2}{\alpha_1}\right|^2 = N_f \sum_{k=0}^{N_f-1} |w_n(\alpha_1)|^2 > N_f \sum_{k=0}^{N_f-1} |w_n(\alpha_2)|^2 = \sum_{k=0}^{N_f-1} \left|\frac{|W_{n,k}(\alpha_2)|^2}{\alpha_2}\right|^2, \tag{25}$$

which leads to (18) and completes the proof of *Lemma* 1.

Lemma 2 *Suppose that* $\{a_n\}$, $\{b_n\}$ *and* $\{c_n\}, n = 0, 1, \ldots, N_f - 1$ *are non-negative real numbers meeting* $\sum_{n=0}^{N_f-1} b_n = \sum_{n=0}^{N_f-1} c_n = 1$, *and* $\sum_{n=0}^{N_f-1} b_n^2 < \sum_{n=0}^{N_f-1} c_n^2$, *we have*

$$\sum_{n=0}^{N_f-1} (b_n \otimes a_n)^2 \leq \sum_{n=0}^{N_f-1} (c_n \otimes a_n)^2. \tag{26}$$

Proof: Since $\sum_{n=0}^{N_f-1} b_n = \sum_{n=0}^{N_f-1} c_n = 1$, and $\sum_{n=0}^{N_f-1} b_n^2 < \sum_{n=0}^{N_f-1} c_n^2$, we have

$$\sum_{n=0}^{N_f-1} \left(c_n^2 - b_n^2\right) = 2 \sum_{i=0}^{N_f-1} \sum_{j=i+1}^{N_f-1} \left(b_i b_j - c_i c_j\right) \tag{27}$$

According to the defination circulant convolution, we have

$$\begin{aligned} &\sum_{n=0}^{N_f-1} (c_n \otimes a_n)^2 \\ &= \left(\sum_{n=0}^{N_f-1} c_n^2\right)\left(\sum_{m=0}^{N_f-1} a_m^2\right) + 2 \sum_{i=0}^{N_f-1} \sum_{j=i+1}^{N_f-1} c_i c_j \sum_{k=0}^{N_f-1} a_k a_{(k+j-i)} \mod N_f \\ &= \left(\sum_{n=0}^{N_f-1} b_n^2\right)\left(\sum_{m=0}^{N_f-1} a_m^2\right) + \left(\sum_{n=0}^{N_f-1} \left(c_n^2 - b_n^2\right)\right)\left(\sum_{m=0}^{N_f-1} a_m^2\right) + 2 \sum_{i=0}^{N_f-1} \sum_{j=i+1}^{N_f-1} c_i c_j \sum_{k=0}^{N_f-1} a_k a_{(k+j-i)} \mod N_f. \end{aligned} \tag{28}$$

Optics EXPRESS

Recall (27), we have

$$\begin{aligned}
&\left(\sum_{n=0}^{N_f-1}\left(c_n^2-b_n^2\right)\right)\left(\sum_{m=0}^{N_f-1}a_m^2\right)\\
=&2\left(\sum_{i=0}^{N_f-1}\sum_{j=i+1}^{N_f-1}(b_ib_j-c_ic_j)\right)\left(\sum_{m=0}^{N_f-1}a_m^2\right)\\
\geq&2\left(\sum_{i=0}^{N_f-1}\sum_{j=i+1}^{N_f-1}(b_ib_j-c_ic_j)\right)\left(\sum_{k=0}^{N_f-1}a_ka_{(k+j-i)\mod N_f}\right),
\end{aligned}\tag{29}$$

and thus,

$$\begin{aligned}
&\sum_{n=0}^{N_f-1}(c_n\otimes a_n)^2\\
\geq&\left(\sum_{n=0}^{N_f-1}b_n^2\right)\left(\sum_{m=0}^{N_f-1}a_m^2\right)+2\sum_{i=0}^{N_f-1}\sum_{j=i+1}^{N_f-1}c_ic_j\sum_{k=0}^{N_f-1}a_ka_{(k+j-i)\mod N_f}\\
&+2\sum_{i=0}^{N_f-1}\sum_{j=i+1}^{N_f-1}(b_ib_j-c_ic_j)\left(\sum_{k=0}^{N_f-1}a_ka_{(k+j-i)\mod N_f}\right)\\
=&\left(\sum_{n=0}^{N_f-1}b_n^2\right)\left(\sum_{m=0}^{N_f-1}a_m^2\right)+2\sum_{i=0}^{N_f-1}\sum_{j=i+1}^{N_f-1}b_ib_j\sum_{k=0}^{N_f-1}a_ka_{(k+j-i)\mod N_f}\\
=&\sum_{n=0}^{N_f-1}(b_n\otimes a_n)^2
\end{aligned}\tag{30}$$

This completes the proof of *Lemma* 2.

Recall (17) that $|G_k|^2$ is in fact the circulant convolution of $\frac{|W_{0,k}|^2}{\alpha}$ and $|H_k|^2$, and thus $\sum_{k=0}^{N_f-1}|G_k(\alpha_1)|^4 > \sum_{k=0}^{N_f-1}|G_k(\alpha_2)|^4$ in the light of *Lemma* 1 and *Lemma* 2, which leads to (14) and completes the proof of the Proposition.

Funding

National Natural Science Foundation of China (61471176); National Key R&D Program of China (2018YFB1801701); Industry-Academia-Research Innovation Project of Blue-Fire of Ministry of Education of the People's Republic of China (CXZJHZ201705); Natural Science Foundation of Guangdong Province (2018A030313990, 2019A1515011940); Science and Technology Planning Project of Guangdong Province (2017A010101015, 2017B030308009, 2017KZ010101); Tip-top Scientific and Technical Innovative Youth Talents of Guangdong Special Support Program (2016TQ03X100); BLUEDON Information Security Technologies Co. (LD20170204, LD20170207).

Disclosures

The authors declare no conflicts of interest.

References

1. Q. Zhang, N. Stojanovic, C. Xie, C. Prodaniuc, and P. Laskowski, "Transmission of single lane 128 Gbit/s PAM-4 signals over an 80 km SSMF link, enabled by DDMZM aided dispersion pre-compensation," Opt. Express **24**(21), 24580–24591 (2016).

Optics EXPRESS

2. K. Zhong, X. Zhou, Y. Wang, J. Huo, H. Zhang, L. Zeng, C. Yu, A. P. T. Lau, and C. Lu, "Amplifier-less transmission of 56Gbit/s PAM4 over 60km using 25Gbps EML and APD," in *Optical Fiber Communication Conference*, (Optical Society of America, 2017), pp. Tu2D–1.
3. S. Ullah, R. Ullah, A. Khan, H. A. Khalid, Q. Zhang, Q. Tian, F. Khan, and X. Xin, "Optical multi-wavelength source for single feeder fiber using suppressed carrier in high capacity LR-WDM-PON," IEEE Access **6**, 70674–70684 (2018).
4. A. Yekani and L. A. Rusch, "Interplay of bit rate, linewidth, bandwidth, and reach on optical dmt and pam with imdd," IEEE Trans. Commun. **67**(4), 2908–2913 (2019).
5. X. Chen, C. Antonelli, S. Chandrasekhar, G. Raybon, J. Sinsky, A. Mecozzi, M. Shtaif, and P. Winzer, "218-Gb/s single-wavelength, single-polarization, single-photodiode transmission over 125-km of standard singlemode fiber using Kramers-Kronig detection," in *Optical Fiber Communication Conference*, (Optical Society of America, 2017), pp. Th5B–6.
6. Z. Li, M. S. Erkılınç, K. Shi, E. Sillekens, L. Galdino, B. C. Thomsen, P. Bayvel, and R. I. Killey, "SSBI mitigation and the Kramers–Kronig scheme in single-sideband direct-detection transmission with receiver-based electronic dispersion compensation," J. Lightwave Technol. **35**(10), 1887–1893 (2017).
7. T. M. Hoang, Q. Zhuge, Z. Xing, M. Sowailem, M. Morsy-Osman, and D. V. Plant, "Single wavelength 480 Gb/s direct detection transmission over 80 km SSMF enabled by Stokes vector receiver and reduced-complexity SSBI cancellation," in *2018 Optical Fiber Communications Conference and Exposition (OFC)*, (IEEE, 2018), pp. 1–3.
8. B. J. Schmidt, A. J. Lowery, and J. Armstrong, "Experimental demonstrations of electronic dispersion compensation for long-haul transmission using direct-detection optical OFDM," J. Lightwave Technol. **26**(1), 196–203 (2008).
9. S. Fu, C. Chen, F. Gao, X. Li, L. Deng, M. Tang, and D. Liu, "Digital chromatic dispersion pre-management enabled single-lane 112 Gb/s PAM-4 signal transmission over 80 km SSMF," Opt. Lett. **43**(7), 1495–1498 (2018).
10. Z. Liu, G. Hesketh, B. Kelly, J. O'Carroll, R. Phelan, D. J. Richardson, and R. Slavík, "Optical injection-locked directly modulated lasers for dispersion pre-compensated direct-detection transmission," J. Lightwave Technol. **36**(20), 4967–4974 (2018).
11. X. Chen, A. Li, D. Che, Q. Hu, Y. Wang, J. He, and W. Shieh, "Block-wise phase switching for double-sideband direct detected optical OFDM signals," Opt. Express **21**(11), 13436–13441 (2013).
12. A. Li, D. Che, X. Chen, Q. Hu, Y. Wang, and W. Shieh, "61 Gbits/s direct-detection optical OFDM based on blockwise signal phase switching with signal-to-signal beat noise cancellation," Opt. Lett. **38**(14), 2614–2616 (2013).
13. J. Armstrong, "OFDM for optical communications," J. Lightwave Technol. **27**(3), 189–204 (2009).
14. J. Zhao and L.-K. Chen, "Adaptively loaded IM/DD optical OFDM based on set-partitioned QAM formats," Opt. Express **25**(8), 9368–9377 (2017).
15. W. A. Ling and I. Lyubomirsky, "Electronic dispersion compensation in a 50 Gb/s optically unamplified direct-detection receiver enabled by vestigial-sideband orthogonal frequency division multiplexing," Opt. Express **22**(6), 6984–6995 (2014).
16. E. Bedeer, O. A. Dobre, M. H. Ahmed, and K. E. Baddour, "Joint optimization of bit and power loading for multicarrier systems," IEEE Wirel. Commun. Lett. **2**(4), 447–450 (2013).
17. O. Narmanlioglu, R. C. Kizilirmak, T. Baykas, and M. Uysal, "Link adaptation for MIMO OFDM visible light communication systems," IEEE Access **5**, 26006–26014 (2017).
18. J. Lian, Y. Gao, and D. Lian, "Variable pulse width unipolar orthogonal frequency division multiplexing for visible light communication systems," IEEE Access **7**, 31022–31030 (2019).
19. B. Yu, C. Guo, L. Yi, H. Zhang, J. Liu, X. Dai, A. P. T. Lau, and C. Lu, "150-Gb/s SEFDM IM/DD transmission using log-MAP Viterbi decoding for short reach optical links," Opt. Express **26**(24), 31075–31084 (2018).
20. I. Darwazeh, T. Xu, T. Gui, Y. Bao, and Z. Li, "Optical SEFDM system; bandwidth saving using non-orthogonal sub-carriers," IEEE Photonics Technol. Lett. **26**(4), 352–355 (2014).
21. J. Huang, Q. Sui, Z. Li, and F. Ji, "Experimental demonstration of 16-QAM DD-SEFDM with cascaded BPSK iterative detection," IEEE Photonics J. **8**(3), 1–9 (2016).
22. J. Zhou, Q. Wang, J. Wei, Q. Cheng, T. Zhang, Z. Yang, A. Yang, Y. Lu, and Y. Qiao, "Faster-than-Nyquist non-orthogonal frequency-division multiplexing for visible light communications," IEEE Access **6**, 17933–17941 (2018).
23. M. Jia, Z. Yin, Q. Guo, G. Liu, and X. Gu, "Waveform design of zero head DFT spread spectral efficient frequency division multiplexing," IEEE Access **5**, 16944–16952 (2017).
24. B. Yu, H. Zhang, X. Hong, C. Guo, A. P. T. Lau, C. Lu, and X. Dai, "Channel equalisation and data detection for SEFDM over frequency selective fading channels," IET Commun. **12**(18), 2315–2323 (2018).
25. B. Yu, L. Yi, C. Guo, J. Liu, X. Dai, A. P. T. Lau, and C. Lu, "Dispersion tolerant 66.7-Gb/s SEFDM IM/DD transmission over 77-km SSMF," in *2018 European Conference on Optical Communication (ECOC)*, (IEEE, 2018), pp. 1–3.
26. S. J. Heydari, M. F. Naeiny, and F. Marvasti, "Iterative detection with soft decision in spectrally efficient FDM systems," arXiv preprint arXiv:1304.4003 (2013).
27. S. Osaki, M. Nakao, T. Ishihara, and S. Sugiura, "Differentially modulated spectrally efficient frequency-division multiplexing," IEEE Signal Process. Lett. **26**(7), 1046–1050 (2019).
28. T. Xu, T. Xu, P. Bayvel, and I. Darwazeh, "Non-orthogonal signal transmission over nonlinear optical channels," IEEE Photonics J. **11**(3), 1–13 (2019).

Optics EXPRESS

29. J. Zhou and Y. Qiao, "Low-PAPR asymmetrically clipped optical OFDM for intensity-modulation/direct-detection systems," IEEE Photonics J. **7**(3), 1–8 (2015).
30. C. Guo, J. Liang, J. Liu, and L. Liu, "Extended reach OFDM-PON using super-Nyquist image induced aliasing," Opt. Express **23**(17), 21798–21808 (2015).
31. P. S. Chow, J. M. Cioffi, and J. A. Bingham, "A practical discrete multitone transceiver loading algorithm for data transmission over spectrally shaped channels," IEEE Trans. Commun. **43**(2/3/4), 773–775 (1995).